Thermochimica Acta, 73 (1984) 67–78
Elsevier Science Publishers B.V., Amsterdam – Printed in The Netherlands

KINETICS AND MECHANISM OF FORMATION OF THE AMORPHOUS PHASE FROM BARIUM CARBONATE AND KAOLIN

Ma. CARMEN GUILLEM VILLAR * and CLAUDIO GUILLEM MONZONÍS

Department of Inorganic Chemistry, Faculty of Chemistry, University of Valencia, Valencia (Spain)

(Received 27 July 1983)

ABSTRACT

The kinetics and mechanism of formation of the amorphous phase from equimolar mixtures of $BaCO_3$ with metakaolin and $BaCO_3$ with kaolin, without mineralizer and with LiF as mineralizer, were studied in a N_2 atmosphere using isothermal thermogravimetric analysis to monitor the fraction of the reaction completed as a function of time between 660°C and 755°C. The identification of the phases present in the fired samples was carried out by X-ray diffraction.

The reactions were found to be diffusion controlled according to the model proposed by Jander. The amorphous phase is produced by diffusion of BaO through the disordered structure of metakaolinite.

The activation energy for the reaction of $BaCO_3$ and kaolin is 62.3 kcal mol^{-1}, the frequency factor being 2.30×10^{10}. The accelerating effect of LiF is clearly shown, not by the activation energy, but by the frequency factor, which for mixture E-2 is 7.89×10^{12}.

INTRODUCTION

When an equimolar mixture of $BaCO_3$ and kaolin are fired progressively, three phases are formed in succession: an amorphous phase and two crystalline phases, hexacelsian and celsian [1].

The purpose of the present work was to elucidate the mechanism of the amorphous phase formation reaction from equimolar mixtures of $BaCO_3$ with kaolin and $BaCO_3$ with metakaolin, as well as the influence of LiF as mineralizer on the reaction kinetics.

The rate of the reaction was indirectly measured by the weight loss due to CO_2 evolution which accompanied the formation of the amorphous phase. Isothermal thermogravimetry was applied, since this technique allows the

* All correspondence should be addressed to: Dra. Ma. Carmen Guillem Villar, Departamento de Química Inorgánica, Facultad de Ciencias Químicas, C/Dr. Moliner no. 50, Burjasot (Valencia), Spain.

0040-6031/84/$03.00

reaction mechanism to be established, whereas non-isothermal thermogravimetry does not [2,3].

The data on fraction of reaction completed as a function of time were used to determine the reaction mechanism, and the rate constants, activation energy and frequency factor were calculated.

THEORETICAL CONSIDERATIONS

Several different types of reaction models have been used to develop mathematical equations describing the kinetics of solid-state reactions in powdered compacts. These fall into four main groups: (1) diffusion models; (2) nuclei growth models; (3) phase boundary models; and (4) models based on the concept of an order of reaction. The rate equations corresponding to the models applied in this study, from the models proposed in the literature, are listed in Table 1, where x is the fraction of reaction completed at time t, k is the rate constant, and t is the reaction time.

The assumptions used in deriving all these rate equations are given by Hulbert [4]. A model is assumed to be correct if the reaction rate constant is independent of time under isothermal conditions. The rate constants in most of the kinetic models of reaction mentioned are a function of the diffusion coefficient. When this is the case, an Arrhenius plot can be used to determine the procedural activation energy of the reaction [5].

TABLE 1

Kinetic models

Name	Equation
Diffusion models	
Jander	$F_J(x) = \{1-(1-x)^{1/3}\}^2 = k_J t$
Kröger–Ziegler	$F_{K-Z}(x) = \{1-(1-x)^{1/3}\}^2 = k_{K-Z} \ln t$
Zhuravlev–Lesokhin–Tempel'man	$F_{Z-L-T}(x) = \left[\frac{1}{(1-x)^{1/3}} - 1\right]^2 = k_{Z-L-T} t$
Ginstling–Brounshtein	$F_{G-B}(x) = 1 - \frac{2}{3}x - (1-x)^{2/3} = k_{G-B} t$
Dunwald–Wagner	$F_{D-W}(x) = \ln\left[\frac{6}{\pi^2(1-x)}\right] = k_{D-W} t$
Nuclei growth models	$F(x) = \ln\frac{1}{1-x} = (kt)^m$
Phase boundary models	
Contracting sphere	$F_{CS}(x) = 1-(1-x)^{1/3} = k_{CS} t$
Contracting disk	$F_{CD}(x) = 1-(1-x)^{1/2} = k_{CD} t$

EXPERIMENTAL

Taking into account the results obtained in previous works [1,6], four mixtures, two of them without addition and the other two with LiF as mineralizer, were prepared (Table 2).

The following materials were used: (a) barium carbonate (C.P. grade); (b) a kaolin, with high kaolinite content, the chemical composition of which (in wt. %) was: SiO_2, 48.4; Al_2O_3, 37.1; Fe_2O_3, 0.4; TiO_2, 0.1; CaO, 0.2; MgO, 0.1; K_2O, 0.5; weight loss at 1000°C, 12.9; (c) metakaolin prepared by prolonged heating of the above kaolin at 600°C, verifying its total dehydroxylation by thermogravimetric analysis; (d) LiF (A.R. grade). Mixtures were thoroughly homogenized in acetone in a planetary ball mill for 1 h.

In all the mixtures (Table 2), the reaction was studied isothermally at 660, 685, 710, 735 and 755°C and times ranging from 6 to 24 h. This sequence was chosen so that at the lowest temperature the dehydroxylation of kaolin was complete and the highest was not high enough for the reaction to take place at an excessive rate.

All the experiments were carried out under the same conditions and in a nitrogen atmosphere using a Setaram instrument which allowed continuous measurement to be made of isothermal weight loss as a function of time. From the recorded weight loss curves the fraction of reaction completed (x for $Al_2O_3 \cdot 2SiO_2 + BaCO_3 \rightarrow Al_2O_3 \cdot 2SiO_2 \cdot BaO + CO_2 \uparrow$) was calculated as the ratio of the weight loss at time t to the theoretical total weight loss.

RESULTS AND DISCUSSION

First of all, some preliminary experiments were made in order to establish that the rate of formation of the amorphous phase could be measured by the change in weight due to CO_2 evolution. This measurement represents the rate of formation of the amorphous phase.

Thermogravimetric analysis of $BaCO_3$ showed that the weight loss due to CO_2 evolution took place between 950°C and 1400°C, the corresponding endothermic peak being produced at 1200°C. However, in the reaction

TABLE 2

Molar compositions of the mixtures studied

Mixture	$BaCO_3$	Kaolinite	Metakaolinite	LiF
A	1	1	–	–
M	1	–	1	–
E-1	1	1	–	0.02
E-2	1	1	–	0.04

between $BaCO_3$ and kaolin, the evolution of CO_2 took place between 660°C and 960°C and the endothermic peak at 815°C [1]. The isothermal thermogravimetry of the equimolar mixture of $BaCO_3$ and kaolin at 755°C showed that the evolution of CO_2 was almost complete in 6 h. No CO_2 evolution was detected from pure $BaCO_3$ for 5 h at 800°C. All these experiments were carried out under the same conditions as the kinetic study.

In a previous work [6], equimolar mixtures of $BaCO_3$ and kaolin were fired isothermally at several temperatures in an electric furnace. The results of X-ray diffraction examination of the samples after each firing showed that at 600°C for 6 h, no kaolinite was detected (i.e., the dehydroxylation of kaolinite had been completed), whereas the $BaCO_3$ pattern remained unchanged; at 900°C for 6 h the amorphous phase was present and no peaks of BaO were discernible. On the other hand, the X-ray diffractograms of pure $BaCO_3$ fired under identical conditions, showed that at 800°C for 6 h the $BaCO_3$ remained unchanged, whereas at 1000°C for 3 h BaO began to be detected. At 1200°C for 6 h, undecomposed $BaCO_3$ was still left.

X-ray diffraction diagrams of the partially reacted samples fired isothermally at temperatures between 660°C and 755°C showed amorphous phase as the product phase and unreacted $BaCO_3$, but no diffraction patterns for BaO were observed. Likewise, the X-ray diagrams of the mixture $BaCO_3$ + kaolin 1 : 1 obtained at temperatures from 500 to 1100°C in 50°C rises did not show peaks of BaO.

All these results indicated that the CO_2 evolution was associated with the reaction between $BaCO_3$ and metakaolin to form an amorphous phase and not with the decomposition of $BaCO_3$ to BaO. Therefore, by measuring the change in weight due to gas evolution, a continuous record of the completed fraction reaction, as a function of time, can be obtained.

Figure 1 shows the effect of temperature on the completed fraction of the reaction as a function of time. Comparison of these curves shows that the reaction of $BaCO_3$ with metakaolin is a little slower than that with kaolin, whereas the accelerating effect of LiF on the reaction rate is much higher for the mixture containing 4 mol % of LiF.

Firstly, a nuclei growth analysis was made for each set of data, and in every case a nonlinear plot resulted. This non-linearity indicates that nuclei growth models are not valid for analyzing the entire reaction. Although for all the mixtures studied the plot of $\ln\{\ln(1/1-x)\}$ vs. $\ln t$ could be broken into two or three straight sections, in every case, these sections neither extended over the same ranges of x nor did the slopes have the same values at all the temperatures for the same mixture, varying from 0.5 to 1. These results indicate that the nuclei growth models do not fit the experimental data in any of the cases. However, rate constants were calculated using the nuclei growth equations with m values within the 0.5 to 1 range, and were plotted against reaction time. The drift observed in rate constants with reaction time further ruled out these models, ratifying the results obtained

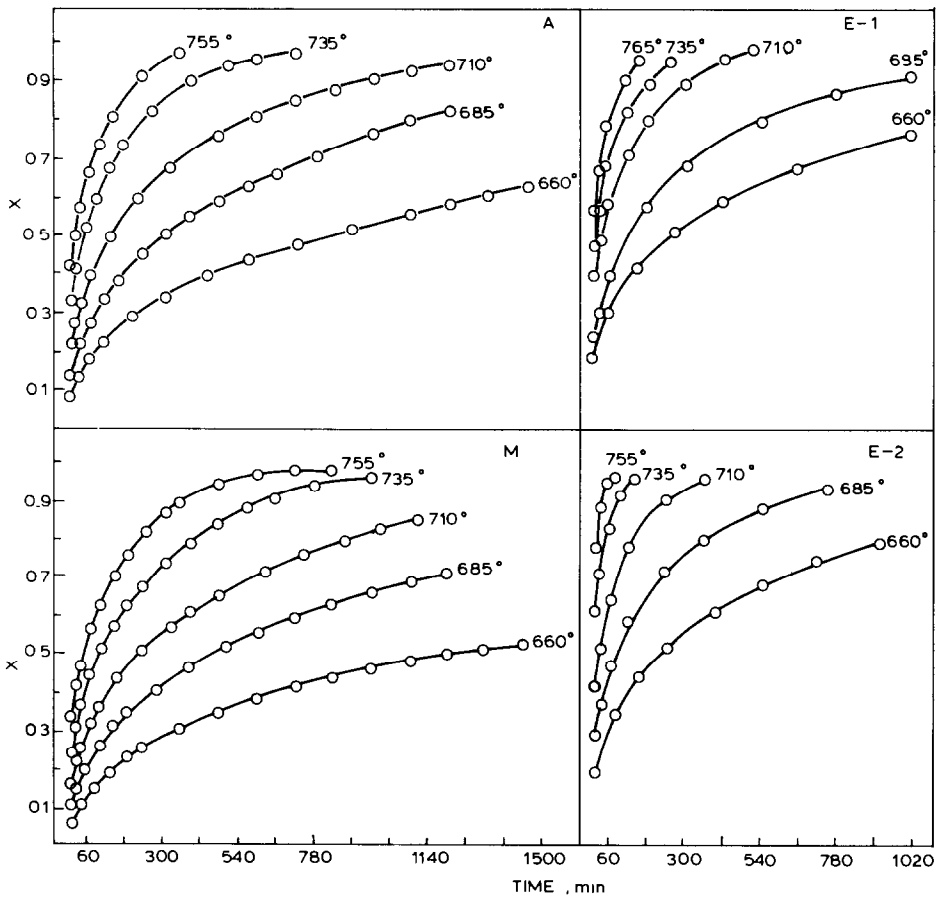

Fig. 1. Isothermal reaction curves for all the mixtures studied.

from the nuclei growth analysis.

The kinetic data (the couples of x–t values) for each set of isothermal reactions were substituted in Jander (J), Kröger–Ziegler (K–Z), Zhuravlev–Lesokhin–Tempel'man (Z–L–T), Ginstling–Brounshtein (G–B), Dunwald–Wagner (D–W), contracting sphere (CS), contracting disk (CD), and nuclei growth (with $m = 1/2, 2/3, 1$) and rate constants were calculated. The rate constants were then plotted as functions of isothermal reaction time (Figs. 2–5). A plot of k against t should result in a horizontal line for the correct model.

For all the mixtures studied, rate constants calculated using the Kröger–Ziegler, Zhuravlev–Lesokhin–Tempel'man, phase boundary and nuclei growth models show a pronounced drift with time (see Figs. 2–5), indicating that these models are not valid for analyzing the amorphous phase formation reaction in solid state from $BaCO_3$ and kaolin. For each mixture the following facts may be emphasized:

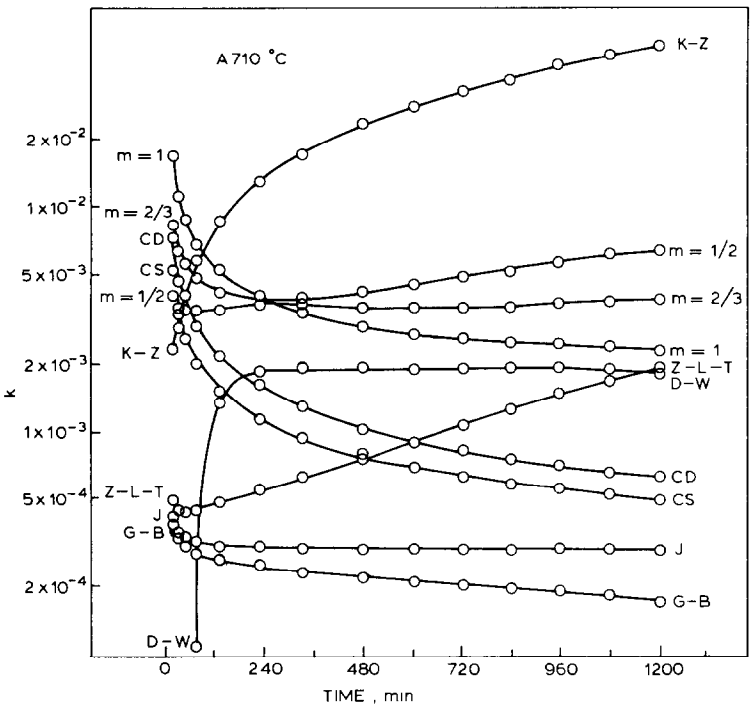

Fig. 2. Analysis of reaction rate equations for the $BaCO_3$ + kaolin reaction at 710°C.

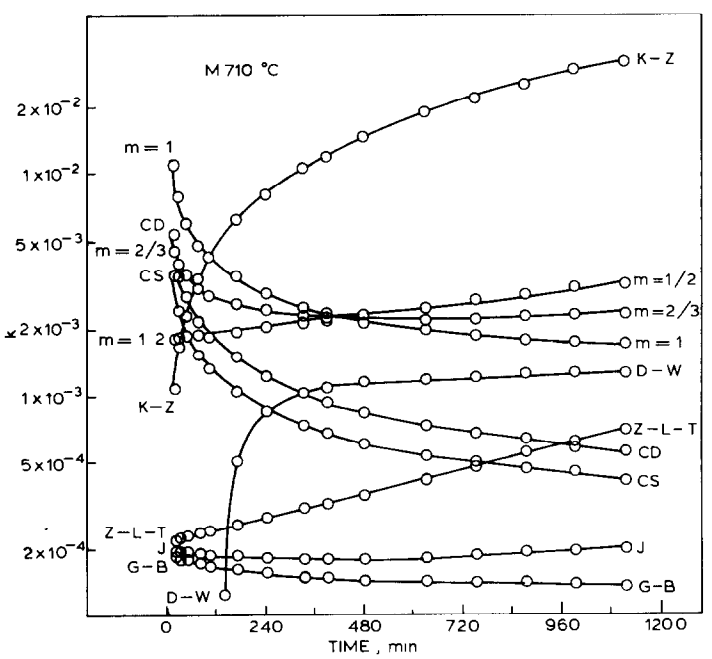

Fig. 3. Analysis of reaction rate equations for the $BaCO_3$ + metakaolin reaction at 710°C

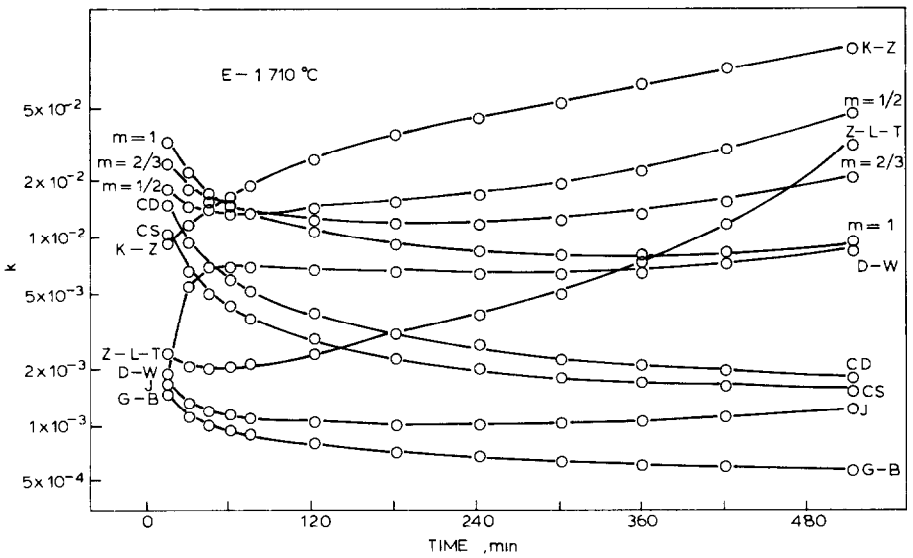

Fig. 4. Analysis of reaction rate equations for the $BaCO_3$ + kaolin mixture, containing 2 mol% LiF, at 710°C.

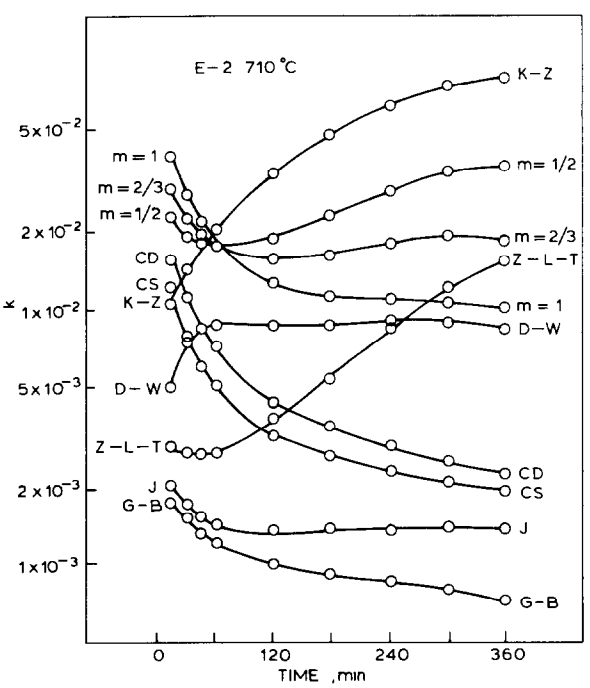

Fig. 5. Analysis of reaction rate equations for the $BaCO_3$ + kaolin mixture, containing 4 mol% LiF, at 710°C.

Mixture A

Rate constants for the reaction between $BaCO_3$ and kaolin without mineralizer (see Fig. 2), calculated using the Jander equation, yield an approximately horizontal plot of rate constant against time. The Dunwald–Wagner model gives a horizontal plot except in the early stage of reaction. Of the other models, the one which shows least drift is the nuclei growth model with $m = 2/3$. For comparison, plots of rate constants calculated, for these three models, against time, were made for each temperature. It was seen that the nuclei growth model drifted considerably from the horizontal plot at almost all temperatures. The Dunwald–Wagner model showed a pronounced drift at 685°C and 660°C. The Jander model was the one which best accomplished the condition of independence of k from t at all temperatures.

The rate constants at each temperature were obtained from the slopes of the straight lines $F(x)_J = \{1-(1-x)^{1/3}\}^2$ vs. t fitted by least-squares analysis. The correlation coefficients (r) and the values of k_J are given in Table 3.

Mixture M

Figure 3 shows that rate constants for the reaction between $BaCO_3$ and metakaolin calculated using the Jander equation yield an approximately horizontal plot of rate constant vs. time. To test the fit of this model to the experimental data, a plot of the rate constants from the Jander model as well as the Ginstling–Brounshtein and Dunwald–Wagner models vs. time was made at each temperature. The D–W model showed a pronounced drift from the horizontal plot at 685°C and 660°C. The G–B model gave a plot near to that of the Jander equation, the differences being higher at 755°C and 735°C.

It can therefore be said that the reaction of amorphous phase formation from an equimolar mixture of $BaCO_3$ and metakaolin (mixture M) takes place through a diffusion mechanism, according to the Jander model, as is also the case in mixture A.

TABLE 3

Correlation coefficients (r) and Jander rate constants (k_J) for mixture A

T (°C)	r	k_J (min^{-1})
755	0.9987	1.30×10^{-3}
735	0.9982	6.79×10^{-4}
710	0.9997	3.06×10^{-4}
685	0.9967	1.57×10^{-4}
660	0.9994	5.38×10^{-5}

TABLE 4

Correlation coefficients (r) and Jander rate constants (k_J) for mixture M

T (°C)	r	k_J (min^{-1})
755	0.9974	7.66×10^{-4}
735	0.9979	4.66×10^{-4}
710	0.9990	1.95×10^{-4}
685	0.9998	9.62×10^{-5}
660	0.9993	3.55×10^{-5}

However, as the G–B model showed behaviour close to that of the Jander model, the values of $F(x)$ from both models were plotted as functions of isothermal reaction time, at each temperature. These plots confirmed that the Jander model was the one which best fitted the experimental data, as the plot of k_J vs. t already made clear. Calculations based on a least-squares analysis for a linear relation between $F(x)_J$ and t yielded the correlation coefficients and the rate constants (k_J) which appear in Table 4.

Mixtures E-1 and E-2

The kinetic models studied in the two cases above were applied to the experimental data of x–t obtained for both mixtures. Rate constants calculated from the corresponding rate equations were plotted as functions of isothermal reaction time (Figs. 4 and 5).

For mixtures E-1 (Fig. 4) and E-2 (Fig. 5) the behaviour is analogous. The Jander model stands out as the one which best fits the experimental data, although the D–W equation also gives a nearly horizontal plot; the G–B model shows a definite slope.

Rate constants calculated using these three diffusion models were plotted against time for all the temperatures. In some cases these plots made it difficult to choose between them. This problem was solved by plotting the values of log k vs. t. For the two mixtures, at all the temperatures, in both plots (k vs. t and log k vs. t) the G–B model drifted from the horizontal as the isothermal reaction time increased. This fact ruled out representation by the G–B model. Of the other two diffusion models preselected, both types of plot indicated that at 710°C the best fit was obtained with the Jander model. At 755°C and 735°C, the two models yielded nearly ideal plots. At 685°C and 660°C, although the k vs. t plot did not allow one of them to be chosen, the log k vs. t plot showed that the Jander model best fitted the experimental data.

In the final result, both models yielded a horizontal plot over a great part of the reaction range, but the D–W model drifted from horizontality for the low values of x to a greater extent than the Jander model.

Plots of $F(x)$ vs. t were made for the two mixtures at all the temperatures,

TABLE 5

Correlation coefficients (r) and Jander rate constants (k_J) for mixture E-1

T (°C)	r	k_J (min^{-1})
755	0.9964	2.90×10^{-3}
735	0.9983	1.72×10^{-3}
710	0.9966	1.06×10^{-3}
685	0.9999	3.35×10^{-4}
660	0.9994	1.48×10^{-4}

using the Jander model. For comparison, $F(x)$ values from the D–W equation were also plotted against time. For both mixtures, although the two models behave in an analogous way at the highest temperatures, the D–W model showed slight drifts from the straight line at 685°C and 660°C, which justified the choice of the Jander model in this case.

Rate constants at each temperature were calculated using the Jander equation. The correlation coefficients and the rate constants, k_J, for mixtures E-1 and E-2 are listed in Tables 5 and 6.

The values of the rate constants (k_J) for the various isothermal reactions calculated at each temperature using the Jander equation (Tables 3–6) were used in constructing Arrhenius plots (Fig. 6). As can be seen in this figure, all the plots fit a straight line. Calculations based on a least-squares analysis

TABLE 6

Correlation coefficients (r) and Jander rate constants (k_J) for mixture E-2

T (°C)	r	k_J (min^{-1})
755	0.932 [a]	6.23×10^{-3}
735	0.9954	3.58×10^{-3}
710	0.9982	1.42×10^{-3}
685	0.9996	5.10×10^{-4}
660	0.9997	1.93×10^{-4}

[a] At 755°C the reaction in mixture E-2 took place at such a rate that caused a scattering of $F(x)$ values.

TABLE 7

Correlation coefficients, activation energies and frequency factors, from the Arrhenius plots of all the mixtures studied

Mixture	r	Activation energy (kcal mol^{-1})	Frequency factor (min^{-1})
A	0.998	62.3	2.30×10^{10}
M	0.999	61.6	9.78×10^{9}
E-1	0.993	60.7	2.49×10^{10}
E-2	0.999	70.9	7.89×10^{12}

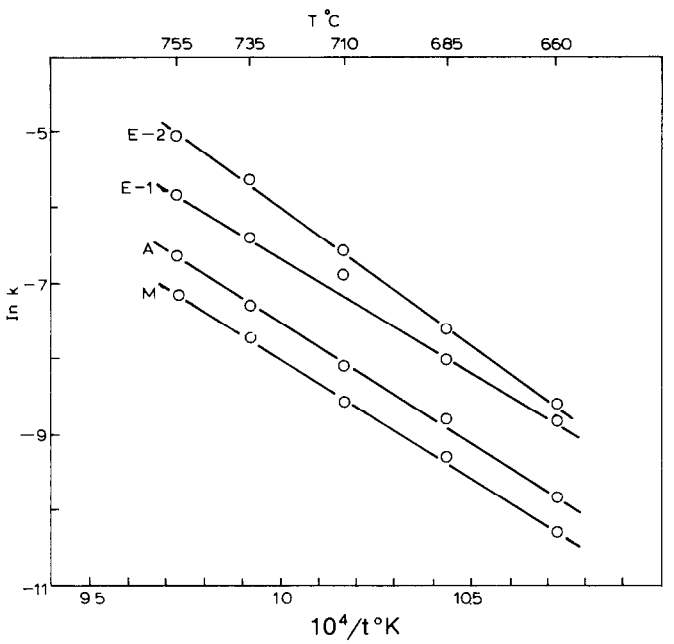

Fig. 6. Arrhenius plots for all the mixtures studied.

for a linear relation between ln k_J and $1/T$ yielded the values of correlation coefficients, activation energies and frequency factors listed in Table 7.

CONCLUSIONS

The amorphous phase formation reaction from an equimolar mixture of $BaCO_3$ and kaolin or metakaolin, without mineralizer and with 2 and 4 mol % of LiF takes place through a diffusion mechanism, according to the model proposed by Jander.

The fact that kaolin in the presence of $BaCO_3$ decomposes in the same way as kaolin alone, and that the mechanism of the reaction is the same whether kaolin or metakaolin are taken as the starting material, show that the dehydroxylation of the kaolin is a step which precedes the amorphous phase formation.

On the other hand, $BaCO_3$ in the mixture (either with kaolin or with metakaolin) decomposes at about 400°C below $BaCO_3$ alone. Furthermore, in the partially reacted samples, unreacted $BaCO_3$ was detected together with the amorphous phase formed, but BaO was not discernible in any of the cases. These results show that the decomposition of $BaCO_3$ occurs due to the reaction of formation of the amorphous phase, which is produced by diffusion of BaO (simultaneous diffusion of Ba^{2+} and O^{2-}) through the disordered structure of metakaolinite.

Table 7 shows the activation energies and frequency factors obtained for all the mixtures studied. The activation energy for the reaction between $BaCO_3$ and metakaolin is slightly lower than that for the kaolin. The activation energy for mixture E-1 is slightly lower than that for mixtures A and M. However, the activation energy for mixture E-2 is higher, whereas the frequency factor is more than 300 times higher than that for mixture E-1. The sequence of frequency factors follows the increasing order M < A < E-1 < E-2. This sequence is the same as that followed by the reaction rates showed in Fig. 1. Therefore, given the direct proportionality between the frequency factor and the reaction rate, it seems that the effect of the mineralizer on the reaction process is made clear by the frequency factor, and thus LiF does not act in reducing the activation energy.

REFERENCES

1 M.C. Guillem Villar, C. Guillem Monzonís and J. Alarcón Navarro, Trans. J. Br. Ceram. Soc., 82 (1983) 69.
2 J.M. Criado and J. Morales, Thermochim. Acta, 19 (1977) 305.
3 B.K. Speronello, C.J. Brinker and W.R. Ott, Thermochim. Acta, 6 (1973) 85.
4 S.F. Hulbert, Trans. J. Br. Ceram. Soc., 6 (1969) 11.
5 W. Gomes, Nature, 192 (1961) 865.
6 M.C. Guillem Villar, C. Guillem Monzonís and V. Lambíes, Bol. Soc. Esp. Cerám. Vidrio, 21 (1982) 239.